

N.I.
CSI

Report No. 453340

Precipitation Scatter Interference Between Space and Terrestrial Communication Systems

F.J. Altman

N68-109361

Prepared Under
Contract NASW 1216

For
National Aeronautics and Space Administration

Communication Systems, Incorporated
Falls Church, Virginia

October 1967

N68-10936
(ACCESSION NUMBER)
56
(PAGES)
02
(CATEGORY)
0290108
(NASA CR OR TMX OR AD NUMBER)

PRECIPITATION SCATTER INTERFERENCE
BETWEEN SPACE AND TERRESTRIAL
COMMUNICATION SYSTEMS

16 October 1967

Contract No. NASW-1216

Prepared by: *F. J. Altman*

F. J. Altman, Director
Advanced Analysis and
Simulation Division

Approved by: *R. M. Hultberg*

for R. M. Hultberg
Vice-President and
Director of Operations

COMMUNICATION SYSTEMS, INCORPORATED
FALLS CHURCH, VIRGINIA

TABLE OF CONTENTS

Section		Page
	SUMMARY	v
1	PROBLEM	1-1
	1.1 General	1-1
	1.2 Specific	1-1
2	GEOMETRY	2-1
	2.1 Elementary	2-1
	2.2 Intersecting Beams	2-2
	2.3 General Case	2-4
	2.4 Simplified Approach	2-5
	2.5 Rough Approximations	2-8
3	METEOROLOGY	3-1
	3.1 Homogeneous Model	3-1
	3.2 Stratiform Model	3-2
	3.3 Thunderstorm Model	3-4
	3.4 Composite Model	3-5
	3.5 Worst Case Estimates	3-11
4	APPROXIMATE METHOD	4-1
	4.1 Concept	4-1
	4.2 Tests	4-2
5	RESULTS	5-1
	5.1 Intersecting Beams - Loss Contours	5-1
	5.2 Intersecting Beams - Loss Profiles	5-3
	5.3 Non-Intersecting Beams	5-8

TABLE OF CONTENTS (Continued)

Section	Page
5.4 Conclusions	5-10
REFERENCES	R-1
Appendix	
A COMPUTATION OF TRANSMISSION LOSS	A-1

LIST OF ILLUSTRATIONS

Figure	Title	Page
2-1	Precipitation Scatter Interference Geometry ..	2-6
2-2	TD-2 Radio Relay Antenna Patterns	2-10
3-1	Reflectivity Profiles for Continuous Precipitation	3-3
3-2	Reflectivity Profiles for Thunderstorms	3-6
3-3	CAPPI Range Intervals	3-7
3-4	Five-Month Reflectivity Profiles	3-9
3-5	Composite Reflectivity Profiles	3-10
3-6	Thunderstorm Days - August	3-12
3-7	Thunderstorm Days - February	3-13
5-1	Loss Contours for Intersecting Beams	5-2
5-2	Effects of Earth's Curvature	5-4
5-3	Loss Profiles for Intersecting Beams	5-5
A-1	Rosman, North Carolina Area	A-3
A-2	Computer Printout	A-4

LIST OF TABLES

Table	Title	Page
3-1	Severe Weather Indices	3-14
4-1	Errors From Geometrical Effects	4-4
5-1	Percentages of Time Initial Refractivity Gradients Are Exceeded	5-6

SUMMARY

The transmission loss is calculated which may be expected from precipitation scatter between earth stations in the space service and microwave radio-relay stations sharing the same frequency band. The geometrical and meteorological factors are developed, including many approximations which permit use of the meager available data to provide rough but valuable siting criteria. It is shown that low altitude beam intersections in most climates give rise to low losses which may cause harmful interference and therefore should be considered in the coordination procedure. The effects of sidelobes may be taken into account in the non-intersecting cases by avoiding intersections of the earth-station beam axis, and cylinders with radii of about six miles centered on the radio-relay station beam axes. Further weather radar data on reflectivity profiles of storms, especially in the tropics, are urgently needed.

LIST OF SYMBOLS

Note: Units are meters or radians unless otherwise stated.
Some subscripts are listed independently.

a	radius of scattering particle
A_e	effective area of antenna
$A_{es,ts}$	azimuth angle of antenna
$b_{es,ts}$	half-power beamwidth of antenna
c	slope of reflectivity profile
d	distance from es to ts
$d_{es,ts}$	distance to scattering volume
$d_{r,t}$	distance to scattering volume
D	d in kilometers
es	<u>earth station</u> in the space service (subscript)
$E_{es,ts}$	elevation angle of antenna
F_s	site-shielding factor in dB
g	gain of antenna
G	gain of antenna in dB
h	height in kilometers
h_b	half-height interval for determination of Z_e
h_o	height of break in bilinear reflectivity profile
h_{ts}	height of terrestrial station
h_x	height of beam intersection
j	intercept of reflectivity profile in km
k	ratio of effective to real earth's radius
K	$(m^2-1)/(m^2+2)$
L_b	basic transmission loss in dB
m	complex index of refraction
N	refractivity = $(n-1)10^6$

p	power
P	power in decibels
Q_s	effective scattering cross section
r	receiver (subscript)
s	distance along beam
S	interference time percentage
t	transmitter (subscript)
ts	<u>terrestrial station</u> in fixed service (subscript)
u	radius of storm core in km
V	scattering volume
x	$2\pi a/\lambda$
y	minimum distance between beams
Z	radar reflectivity factor per unit volume in mm^6/m^3
Z_e	effective value of Z
Z_o	surface value of Z
α	angle from beam axis
η	reflectivity per unit volume
θ	scatter angle between beams
λ	wavelength
σ	back-scattering cross section

SECTION 1

PROBLEM

1.1 GENERAL

Both space and terrestrial services have been assigned frequencies in the same parts of the 1- to 10-GHz band because of a common need for wide bands suitable for line of sight propagation. To make this sharing practical and advantageous, the CCIR has been developing policies to insure tolerable interference with minimum restriction on the parties involved. In the case of propagation between earth stations in the space service and conventional radio-relay stations, only tropospheric propagation along the intervening great-circle path has been considered by the CCIR in detail. The interference is defined in terms of power exceeded 0.01 percent of the time, and site shielding from a ring of hills, for example, has been assumed to provide protection.

1.2 SPECIFIC

It is known, however, that the scattering of radio waves from precipitation is quasi-isotropic, as discussed in the following, so that harmful interference may arise from directions well off the great-circle path, and along the great-circle path even in spite of shielding effective against only conventional forward scatter, which is critically dependent on low launch angles. This was first demonstrated by Doherty (Reference 1) and analyzed by Dennis (Reference 2). More recently, NASA has supported experiments (Reference 3) for verification by ESSA/ITSA (CRPL) of the reality of the problem, and the present study to determine the distribution of precipitation scatter interference in time and space.

SECTION 2

GEOMETRY

2.1 ELEMENTARY

If a homogeneous isotropic medium and certain terminology are assumed, the meteorological aspects may be deferred and the geometry attacked independently. For a small scattering volume element, using meters and radians except as noted,

$$dp_r = dp_s A_e / 4\pi d_r^2 = dp_s g_r \lambda^2 / (4\pi d_r)^2 \quad (2-1)$$

where dp_r = power received at distance d_r

dp_s = power scattered isotropically

A_e = effective receiving antenna area

g_r = effective antenna gain

λ = wavelength = 300/frequency in MHz

But

$$dp_s = Q_s p_t g_t / 4\pi d_t^2 \quad (2-2)$$

where Q_s = total effective scattering cross section

p_t = power transmitted at distance d_t

g_t = effective transmitting antenna gain

Also,

$$Q_s = ZdV / 3.6 \times 10^{15} \lambda^4 \quad (2-3)$$

where dV = scattering volume element

Z = radar reflectivity factor (Reference 6) per unit volume in mm^6/m^3

= $\eta \times 3.6 \times 10^{15} \lambda^4$ for Rayleigh scattering

$\eta = Q_s / V$ = reflectivity per unit volume

Combining the preceding, the transmission loss is

$$p_r/p_t = \frac{1}{.71 \times 10^{19} \lambda^2} \int \frac{g_r g_t Z}{d_r^2 d_t^2} dV \quad (2-4)$$

2.2 INTERSECTING BEAMS

To derive a simple expression for the volume common to two intersecting beams, it is useful at this point to recognize that the earth-station antenna is usually much larger than that of the terrestrial radio-relay station, and that its elevation angle is usually much higher than the latter's so that its beam diameter at the common volume will be much smaller. Then the volume may be considered as a cylinder of diameter defined by the earth-station antenna half-power beamwidth, b_{es} , and for generality, of a length s along this cylinder, which may depend on the larger beamwidth or on the meteorological model.

Thus, with $V = \pi(b_{es} d_{es})^2 s / 4$ and the relationship $g_{es} b_{es}^2 = \pi^2$ (Reference 4), where d_{es} and g_{es} are the distance from and gain of the earth-station antenna, it is found that

$$p_r/p_t = g_{ts} Z s / 10^{19} \lambda^2 d_{ts}^2 \quad (2-5)$$

where transmission now may be in either direction, but g_{ts} and d_{ts} are the gain of, and the distance from the scattering volume to, the terrestrial radio-relay station. If the two beams intersect in a homogeneous medium, then approximately

$$s = d_{ts} b_{ts} / \sin \theta \quad (2-6)$$

where b_{ts} is the radio-relay station 3-dB beamwidth and θ is the scatter angle between the beams.

Using $g_{ts} b_{ts}^2 = \pi^2$, it is seen that in this case

$$p_r/p_t = Z/10^{17} \lambda^2 b_{ts} d_{ts} \sin \theta \quad (2-7a)$$

$$= Z/10^{17} \lambda^2 b_{ts} d \sin \theta_{es} \quad (2-7b)$$

by the law of sines, where d is the separation and θ_{es} the angle between the great-circle path and the line from the earth station to the scattering volume. If the medium is not homogeneous, but Z follows a bilinear profile as indicated in Paragraph 3.4, an equivalent factor, Z_e , may be used as derived in the following using h and D in kilometers.

If the beams intersect at height h_x , in an atmosphere with refractivity gradient corresponding to an effective earth's radius k times the real radius, the smaller beam leaves the larger approximately at height $h_x + h_b$ where E_{es} is the earth-station beam elevation, and

$$2h_b = D_{ts} b_{ts} \sin \tan^{-1} [\tan E_{es} / \sin \cos^{-1} (\cos \theta / \cos E_{es})] \quad (2-8)$$

Then

$$Z_e = \frac{1}{2h_b} \int_{h_1}^{h_2} Z(h) dh \quad (2-9)$$

$$\begin{aligned} \text{where } h_1 &= h_x - E_{ts} D_{ts} & \text{if } E_{ts} D_{ts} < h_b \\ &= h_x - h_b & \text{if } E_{ts} D_{ts} \geq h_b \\ h_2 &= h_x + h_b \end{aligned}$$

The integral is divided by $2h_b$ instead of $h_2 - h_1$ because Equation (2-7a) uses a volume double what it should be when the radio-relay beam axis is on the horizon for $E_{ts} = 0$.

For the bilinear profile of Paragraph 3.4,

$$Z(h) = \exp 2.3(h-j)/c \quad \text{or} \quad \log Z(h) = (h-j)/c \quad (2-10)$$

$$\text{where } c = c_2 \quad h \geq h_0 \text{ km}$$

$$c = c_1 \quad h \leq h_0 \text{ km}$$

and h_0 = bilinear break height.

Integrating Equation (2-9), when both h_1 and h_2 lie above or below h_0 ,

$$2h_b Z_e = (c_1/2.3)[Z(h_2) - Z(h_1)] \quad h \leq h_0 \quad (2-11)$$

$$= (c_2/2.3)[Z(h_2) - Z(h_1)] \quad h \geq h_0 \quad (2-12)$$

When h_0 lies between h_1 and h_2

$$2h_b Z_e = (c_2/2.3)[Z(h_2) - Z(h_0)] + (c_1/2.3)[Z(h_0) - Z(h_1)]$$

2.3 GENERAL CASE

In the general case the beam axes do not intersect, and there may be no volume common to the 3-dB beam cones. This case is treated by computing the transmission loss between the main beam of each terminal and the sidelobes of the other in turn, ignoring that between the sidelobes of one and those of the other, as this contribution can be shown to be negligible. If the 3-dB beam cones intersect, this common volume should be included in only one of the two integrations, not both. In one direction, the relatively high-angle earth-station main lobe may be subdivided into lengths ds , and then g_{ts} , Z , and d_{ts} considered as functions of s . In this case, from Equation (2-5).

$$(p_r/p_t)_{e.s.} = \int_{s_1}^{s_2} \frac{g_{ts}(s)Z(s)}{10^{18} \lambda^2 d_{ts}^2(s)} ds \quad (2-13)$$

Here, s_1 is the distance from the earth station to the lowest point of the volume of interest, defined by the intersection of the tangent plane through the terrestrial radio-relay station. In either case, the heights of the stations and the surrounding terrain may require consideration, as may the effective earth's radius. Their effects are clearly most important at long ranges, as shown in Paragraph 5.2. The upper limit may be determined by the top of the meteorological model, at an altitude of 20 kilometers, for example.

In the other direction, the relatively low-angle terrestrial station main lobe is divided into segments, using the appropriate form of Equation (2-5) considering the terrestrial station antenna beam as a cone,

$$(p_r / p_t)_{t_s} = \int_{s_1}^{s_2} \frac{g_{e,s}(s)Z(s)}{10^{18} \lambda^2 d_{e,s}^2(s)} ds \quad (2-14)$$

Now, s_1 is the distance from the terrestrial station along its beam to the tangent plane through the earth station. The upper limit may be set for computation economy at a distance beyond which the integral is negligible. As the reflectivity varies in the nearly vertical volume element, the Z_e of Paragraph 2.2 should be used with

$$h_b = D_{ts} b_{ts} / 2 \quad (2-15)$$

2.4 SIMPLIFIED APPROACH

A useful simplified expression for integration along the earth-station beam may be derived from Equation (2-13) by using the facts that the terrestrial radio-relay beam elevation is always very small, and that the earth-station beam elevation is often 30° or more. Typical configurations are sketched in orthogonal projections in Figure 2-1 for an earth-station elevation of

30° and various azimuths. It may be seen that for a separation of 300 km and a typical terrestrial radio-relay station beamwidth of 2°, d_{ts} is closely equal to d . When the terrestrial station main beam is not aimed within a few beamwidths of intersection with the earth-station beam, its sidelobes may be considered to have constant gain, g_{ts} , over the limited angle subtended by the effective lower portion of the latter. If now $ds = (1000/\sin E_{es})dh$ is used, where E_{es} is the elevation of the earth station; then

$$(p_r/p_t)_{es} = \frac{g_{ts}}{10^{15} \lambda^2 d^2 \sin E_{es}} \int_{h_1}^{h_2} Z(h) dh \quad (2-16)$$

where h_1 and h_2 are the heights of the intersections at s_1 and s_2 as discussed in the previous paragraphs.

A simplified expression for integration along the terrestrial station beam may also be derived, using Equation (2-14). It is again convenient to assume a highly elevated earth-station antenna beam, an equivalent reflectivity factor, and a terrestrial station antenna beam throughout which g_{es} is constant. With these assumptions and the law of cosines, Equation (2-14) becomes

$$(p_r/p_t)_{ts} = \frac{Z_e g_{es}}{10^{15} \lambda^2} \int_{s_1}^{s_2} \frac{ds}{d_{es}^2} \quad (2-17)$$

$$= \frac{Z_e g_{es}}{10^{15} \lambda^2} \int_{s_1}^{s_2} \frac{ds}{s^2 + d^2 - 2sd \cos \alpha_{ts}} \quad (2-18)$$

where α_{ts} is the angle between the terrestrial antenna beam and the direction toward the earth station. Integrating

$$(p_r/p_t)_{ts} = \frac{Z_e g_{es}}{10^{15} \lambda^2 d \sin \alpha_{ts}} \left[\tan^{-1} \left(\frac{s}{d \sin \alpha_{ts}} - \cot \alpha_{ts} \right) \right]_{s_1}^{s_2} \quad (2-19)$$

2.5 ROUGH APPROXIMATIONS

As the chief interest in precipitation scatter is in its avoidance, it is not so important to provide exact measures of its amount as useful guides regarding undesirable configurations. This is clearly difficult to do accurately, but rough criteria are valuable if they are easy to apply and are not too restrictive.

From Equation (2-13), with the assumptions in Equation (2-16) and the use of an effective reflectivity factor,

$$(p_r/p_t)_{e.s.} = g_{ts} Z_e s / 10^{18} \lambda^2 d_{ts}^2 \quad (2-20)$$

Figure 2-2, taken from Curtis (Reference 5), shows that the approximation

$$\begin{aligned} g_{ts} &= 0.31/\alpha_{ts}^2 \quad (\alpha \text{ in radians}) \\ &= 1000/\alpha_{ts}^2 \quad (\alpha \text{ in degrees}) \end{aligned} \quad (2-21)$$

fits the paraboloid and lens antenna patterns fairly well between 4° and 60° and is higher than that of the horn antenna.

Now in this case α_{ts} is the angle toward an element of the earth-station beam. This is a minimum in the region of closest approach of the beams. Thus Z_e should be found in this region, $\alpha_{ts} d_{ts}$ is the distance between beams, y , and

$$(p_r/p_t)_{e.s.} = 3.1 \times 10^{-19} Z_e s / \lambda^2 y^2 \quad (2-22)$$

If α_{ts} is 30° or less, and $\alpha_{ts} d$ is again recognized as y then Equation (2-19) becomes

$$(p_r/p_t)_{ts} = \frac{Z_e g_{e.s.}}{10^{18} \lambda^2 y} \left[\tan^{-1}(s-d)/y \right]_{s_1}^{s_2} \quad (2-23)$$

If the gain everywhere along the terrestrial antenna beam is constant, for example, 0.1, and if $d \gg y$, then effectively $s_1 = 0$, $s_2 = \infty$ and

$$(p_r/p_t)_{t_s} = 3.1 \times 10^{-19} Z_e / \lambda^2 y \quad (2-24)$$

If desirable, a more appropriate, higher gain can be used over the limited portion of the terrestrial antenna beam passing nearest the earth station, using estimated values of s_1 and s_2 .

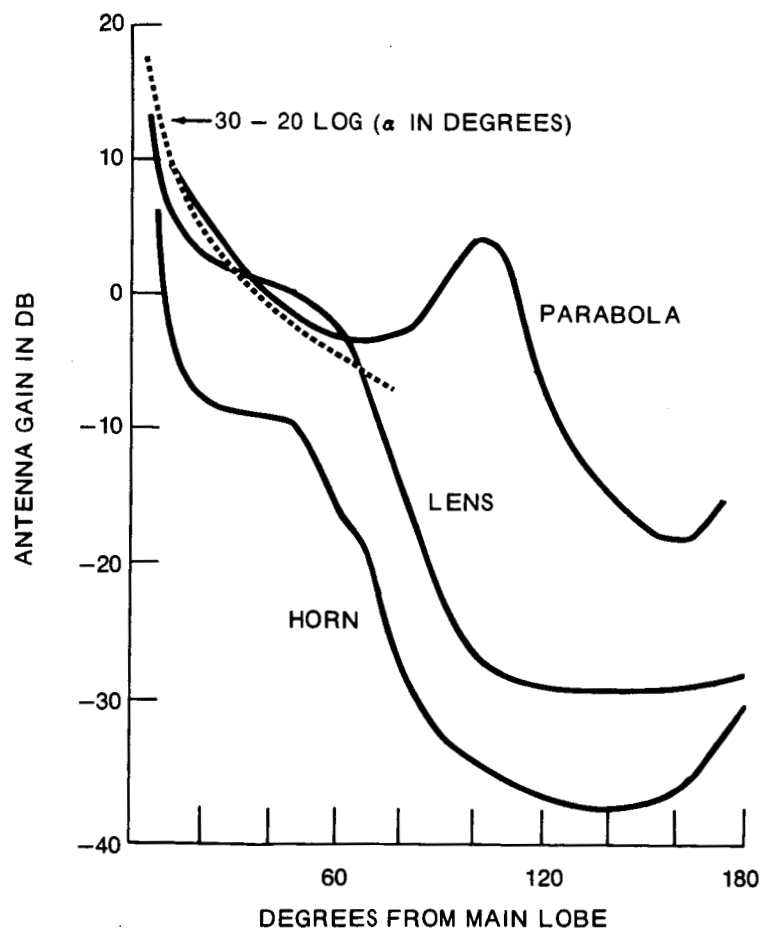


Figure 2-2. TD-2 Radio Relay Antenna Patterns

SECTION 3

METEOROLOGY

3.1 HOMOGENEOUS MODEL

As radar back-scatter data will be used as a measure of side or off-path scatter, it is important to know the relationship between them. Because this is a difficult matter, it will be concisely summarized although the material is readily available elsewhere (see Reference 6). When the radius of a scattering particle, a , is small with respect to the wavelength, that is, $x = 2\pi a/\lambda \ll 1$, then the ratio of the back-scattering cross section σ to the geometrical cross section is

$$\sigma/\pi a^2 = 4x^4 |K|^2 \quad (3-1)$$

where $|K|^2$ is approximately 0.93 for water and 0.20 for ice. The equation does not hold beyond $x = 0.3$, but at $\lambda = 5$ cm this corresponds to a raindrop diameter of 4.8 mm, a size rarely exceeded. It is the radiation pattern, however, which is of most interest, and up to about $x = 0.5$ this is like that of a dipole, with nulls in the direction of the electric vector and omnidirectional perpendicular thereto, with a gain of 3/2. Thus, rain is quasi-isotropic in the horizontal plane if the radiator is vertically polarized.

The large ice particles found high in most thunderstorms, on the other hand, exhibit very complex behavior. Dry ice spheres scatter more strongly than water for $x > 2$, but this may be reduced by a wet or spongy surface or a spongy interior. The radiation patterns may be accentuated by departures from sphericity or smoothed by the presence of a range of sizes, but both

theory and experiment indicate a quasi-isotropic pattern independent of polarization, strongest in the forward direction, with back-scatter roughly about 5 dB below the average side scatter (Reference 3). Although this implies that 5 dB should be added to the interference values computed in the following, the correction will not be made as it applies only to the large particles found in thunderstorms, not to other forms of precipitation, and it is offset partially by a negative 1.4-dB correction discussed by Probert-Jones (Reference 4).

In measuring Z at highly-attenuated frequencies such as X-band, a correction must be made for precipitation not seen due to intervening precipitation. After a model is constructed using corrected data, it must be used with the same phenomenon in mind. At the highest reflectivities, the common volume may be reduced by attenuation in the nearest portion, an effect which is not normally important in the 4- and 6-GHz bands of most interest here.

3.2 STRATIFORM MODEL

The meteorologist recognizes two main types of precipitation. The simplest is called continuous - either rain or snow from a stratiform cloud structure which is uniform over a large area and relatively limited in height. Atlas (Reference 7) gives model profiles for stratiform summertime rain which may be approximated as in Figure 3-1:

$$h = 6.8 \log (Z_0/Z) \qquad h < 4.5 \text{ km} \quad (3-2a)$$

$$h = 1.4 \log (Z_0/Z) + 3.5 \qquad h > 4.5 \text{ km} \quad (3-2b)$$

$$\text{or by } \log Z = \log Z_0 - 0.05 h^2 \qquad (3-2c)$$

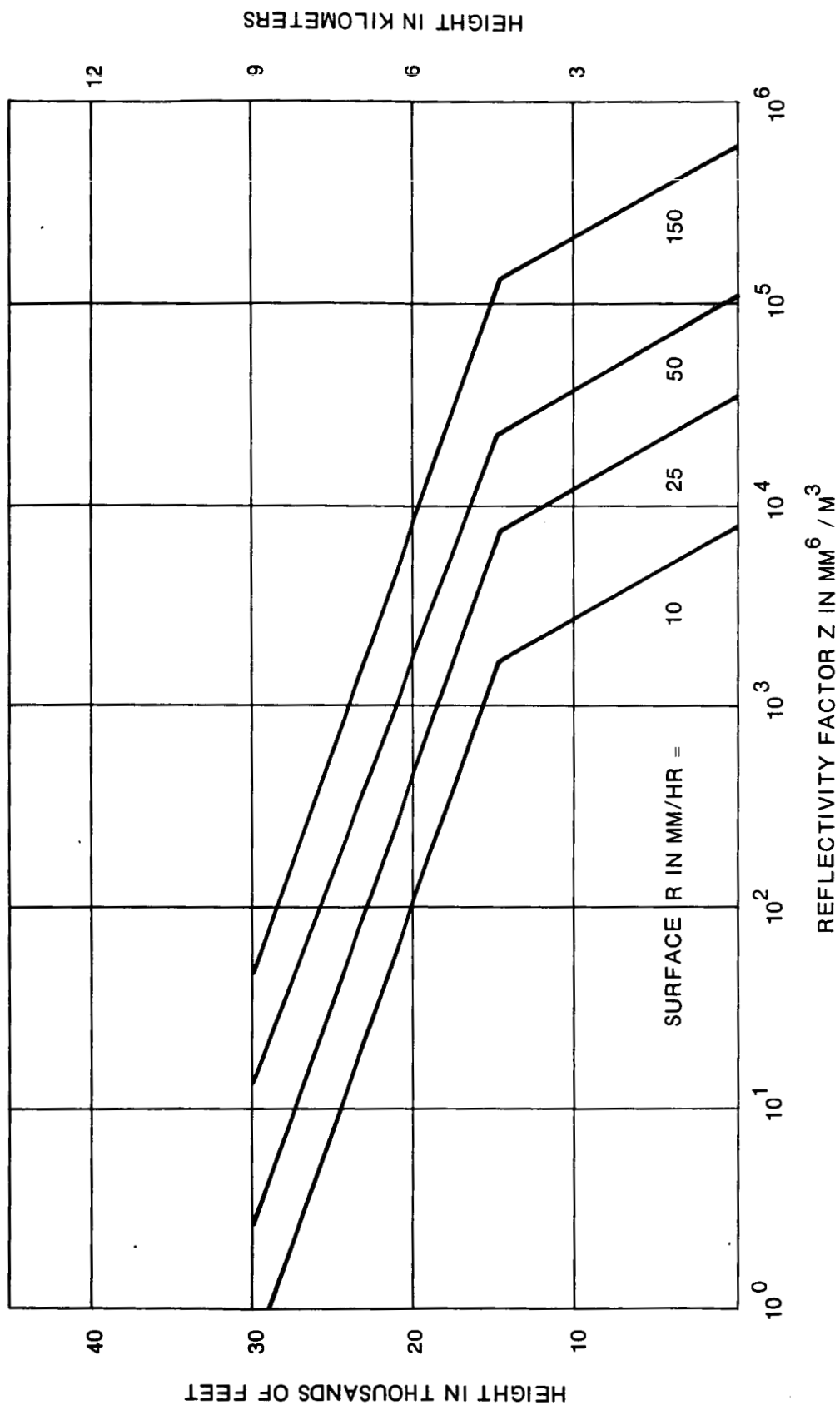


Figure 3-1. Reflectivity Profiles for Continuous Precipitation

where Z_0 = reflectivity factor at the surface, usually considered related to the rainfall rate R in mm/hr by

$$Z = 200R^{1.6} \text{ mm}^6/\text{m}^3 \quad (3-3)$$

For Washington, D.C., Bussey (Reference 8) shows about one hour a year at a rate of 25 mm/hr or more ($Z_0 = 3.4 \times 10^4$ for 0.14 percent of a month), and for the U.S. about five minutes once in two years at a rate of 150 mm/hr ($Z_0 = 6 \times 10^5$ for 0.01 percent of a month). Rain fell at the latter rate in Washington, D.C., in 1963 although it is more likely to occur along the eastern Gulf Coast. As an indication of possible rainfall, Figure 5-5 of Reference 7 shows 12 inches of rain in 40 minutes at Holt, Missouri, on June 22, 1947, corresponding to a rate of 450 mm/hr for about 0.1 percent of a month. In this paper the effect of the "bright band" is ignored. This is an enhanced return from wet snow near the 0°C isotherm, often at about 2- to 3-km altitude in the summer in Montreal.

3.3 THUNDERSTORM MODEL

The more complex type of precipitation is called showery or convective. It is not uniform in time or space like the continuous model, rapidly varying over small areas due to its turbulent origin. If the development reaches eight or nine kilometers in height it normally becomes a thunderstorm, with strong updrafts repeatedly carrying precipitation to great heights, usually becoming hail because of the cold. Thus the largest particles occur at the greatest heights, within free-space ranges of many hundreds of miles from earth and terrestrial stations. Because thunderstorms are so important they will be characterized in several ways: cell descriptions, cell reflectivity profiles, and overall reflectivity profiles.

The classic study (Reference 9) of 199 Ohio thunderstorms during 1949 indicates the following regarding the component cells:

- a. The cell diameter is roughly equal to its height.
- b. Over 60 percent extended above 10 km.
- c. The percentage coverage at 10 km is about 3 percent on the average and 11 percent maximum.
- d. The mean duration is approximately 25 minutes.

Donaldson (Reference 10) has published reflectivity profiles representing 42 severe storms, observed during two years from a CPS-9 radar in the Boston area. From these, about four storms a year may be characterized as having a maximum Z at 9 km and a core Z of 10^6 at 6 km, leading to a rough estimate of maximum likely $\int Z(h)dh$ of about $10^6 \times 10 = 10^7$, consistent with Donaldson's later storm models. As shown in Figure 3-2 from Donaldson, thunderstorm cores generally have Z profiles that do not fall off rapidly with height. It is this which renders site shielding ineffective wherever thunderstorms are common. As a storm normally consists of a group of cells each less than 16 km in diameter and of varying height, it is difficult to estimate total reflectivity distributions in time and space.

3.4 COMPOSITE MODEL

The model that has been adopted for most of these studies is a composite one including all the precipitation for several months, sampled regularly in time and space by a specially-equipped weather radar (Reference 11). It uses the constant-altitude PPI (CAPPI) principle, illustrated in Figure 3-3, successively sweeping the sky at increasing elevations, gating the video signal so that the display tube maps the reflectivity at several heights in succession. By photographing the display at regular intervals, scanning the photos and using the resulting signals to trigger a series of time-measuring circuits with appropriate thresholds, profiles are obtained which show versus height, the percentage of area on a given picture above each

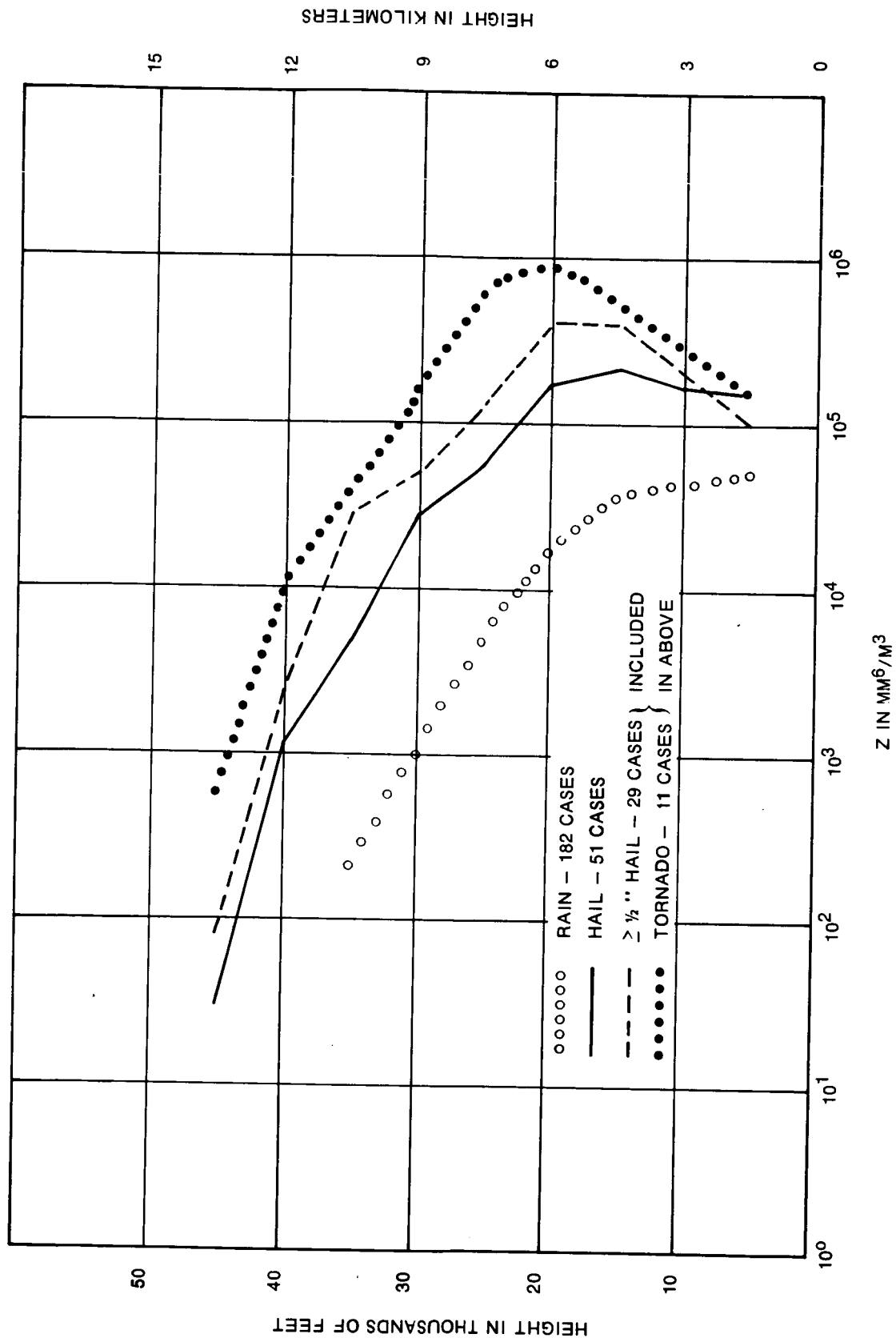


Figure 3-2. Reflectivity Profiles for Thunderstorms

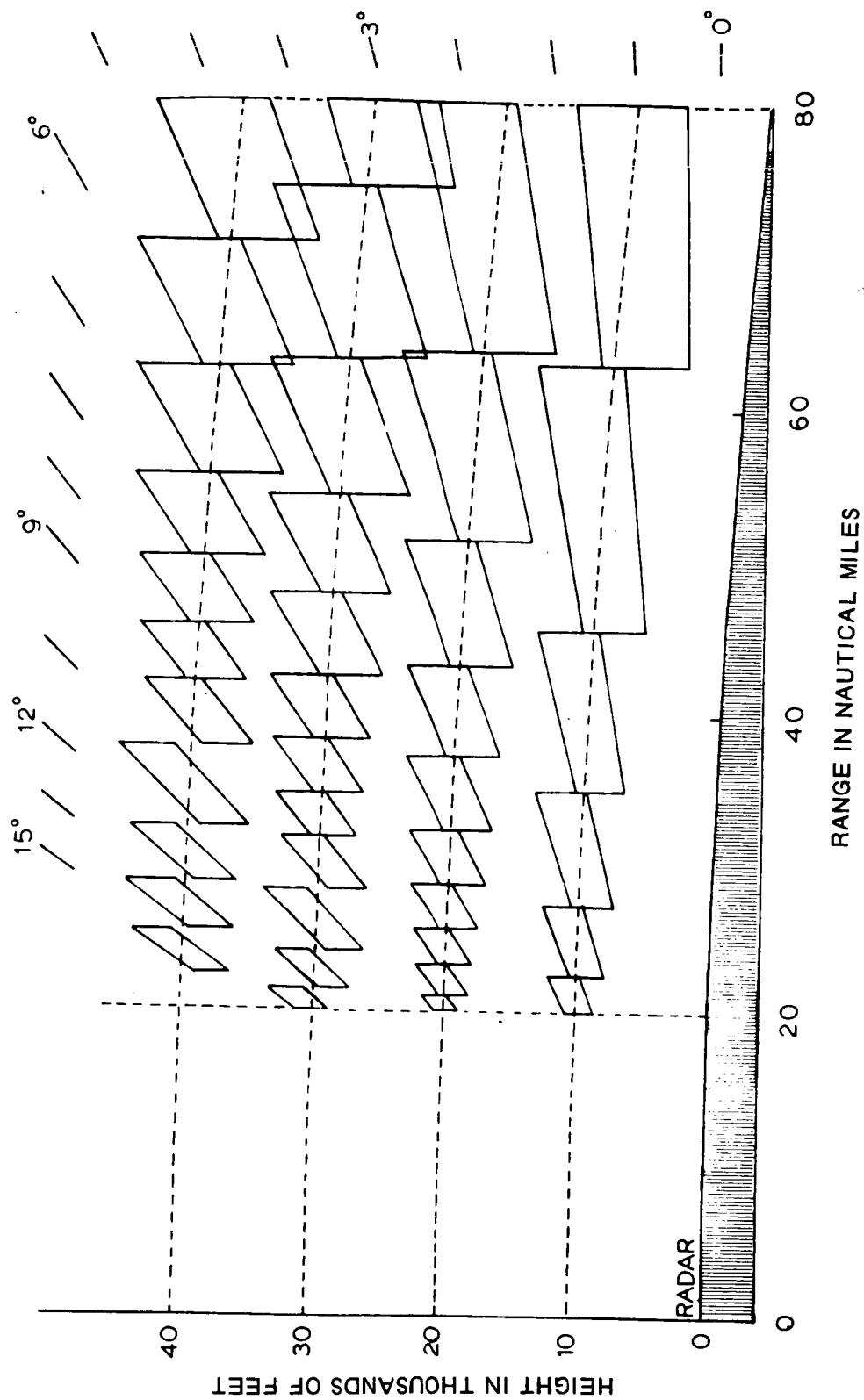


Figure 3-3. CAPPI Range Intervals

threshold. These profiles may be summed from May through September as in Figure 3-4 from Marshall et al (Reference 12) to give a composite representing an entire summer. The thresholds, corrected for attenuation at X-band, are:

Thresh-							
old	(1)	(2)	(3)	(4)	(5)	(6)	(7)
Z	5×10^0	4.6×10^1	4.2×10^2	3.8×10^3	3.5×10^4	3.2×10^5	2.9×10^6

The abscissas are in terms of nautical miles²-hours, where the maximum is 7.2×10^7 , the product of the 20,000-nautical mile² area on each picture and the 3600 hours in five months. If then it is assumed that the region observed is uniform in regard to precipitation distribution, a reflectivity profile representing 0.01 percent of the time can be found by making a vertical section at 7.2×10^3 nautical miles² hours. In this way points have been plotted on Figure 3-5 and then fitted with bilinear equivalents for ease in use with a computer. The expressions for 0.01 percent of the five months are

$$\begin{aligned} h &= -5 \log Z + 26 & h < 6 \text{ km} \\ h &= -2.3 \log Z + 15.2 & h > 6 \text{ km} \end{aligned} \quad (3-4)$$

As interference criteria are expressed in terms of percentage of any month, the original data were inspected and this profile found to apply for 0.02 percent of the worst month.

The use of data in the form described involves an assumption that the reflectivity of interest does not vary greatly in the horizontal direction within the volume element. An inspection of detailed reflectivity distributions in storm cells indicates that this assumption is not likely to be closely true for the highest reflectivities and the largest volumes. However, from Figure 3-4, the profile for 0.01 percent of the total does not involve reflectivities above 3.5×10^4 , with the lower-valued, more uniform, distributions at the greater heights. Thus it is seen even at long ranges, with large, high common volumes, that appreciable errors are unlikely, and that for shorter ranges, or

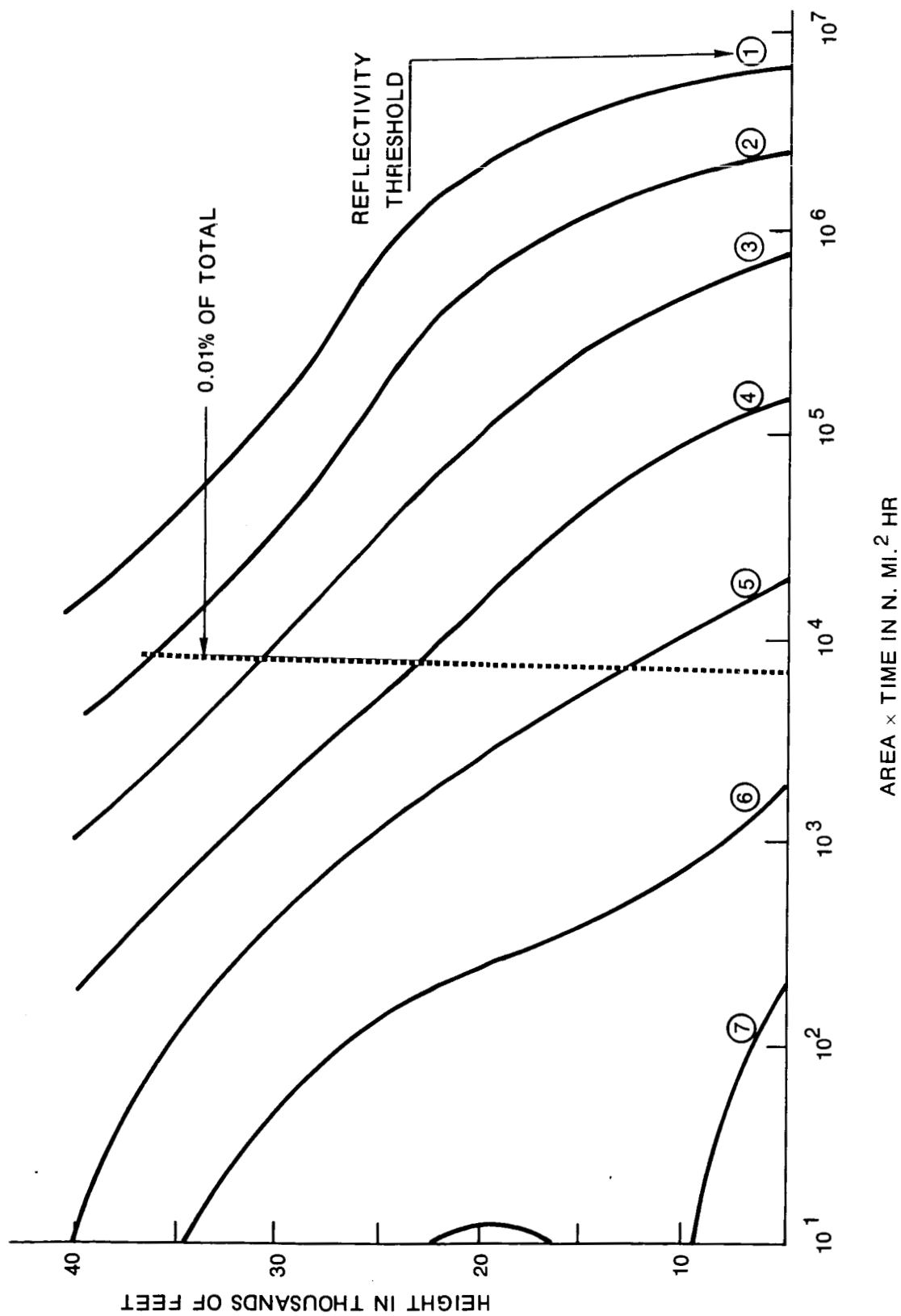


Figure 3-4. Five-Month Reflectivity Profiles

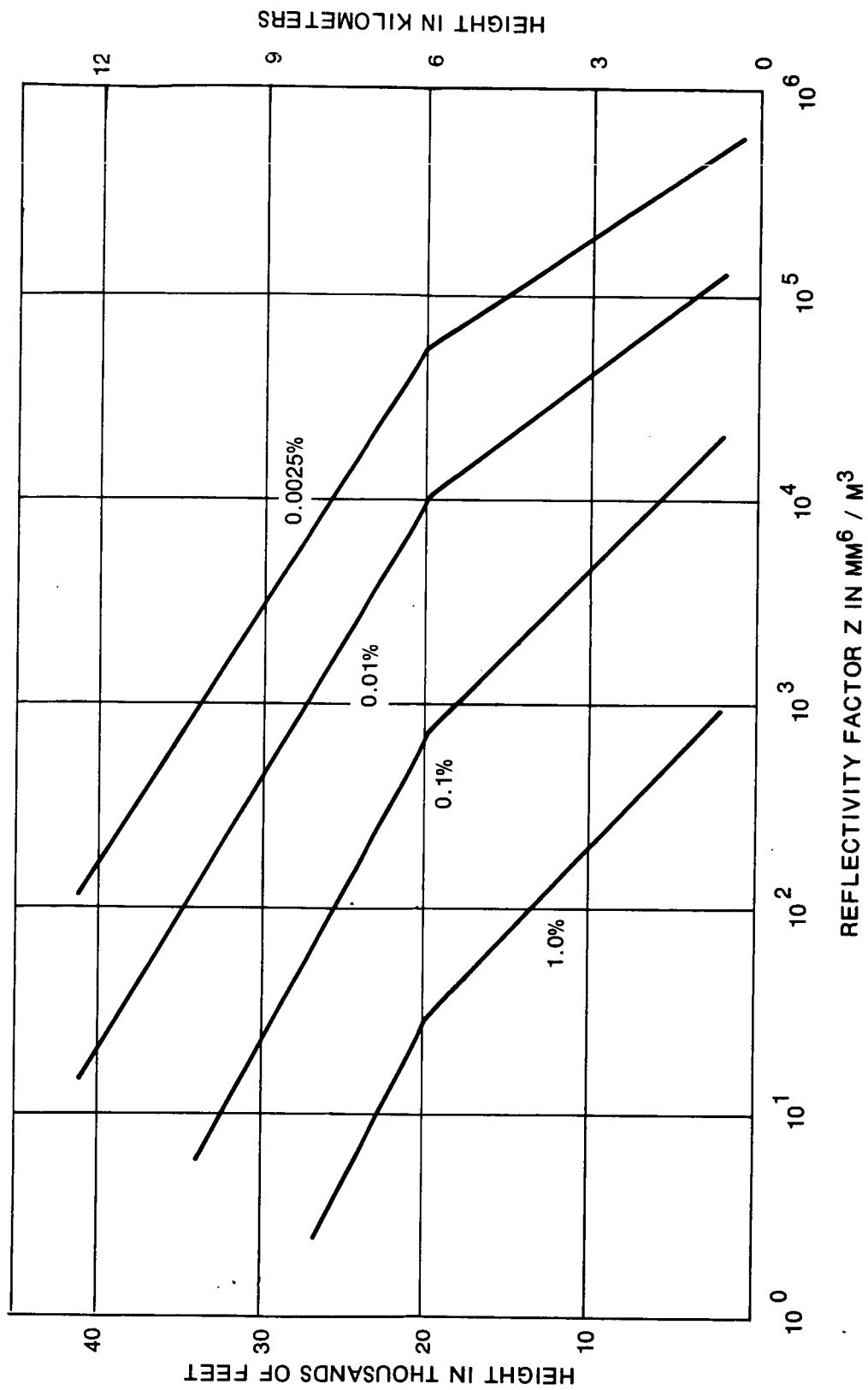


Figure 3-5. Composite Reflectivity Profiles

for relatively uniform continuous precipitation, the effects are very small.

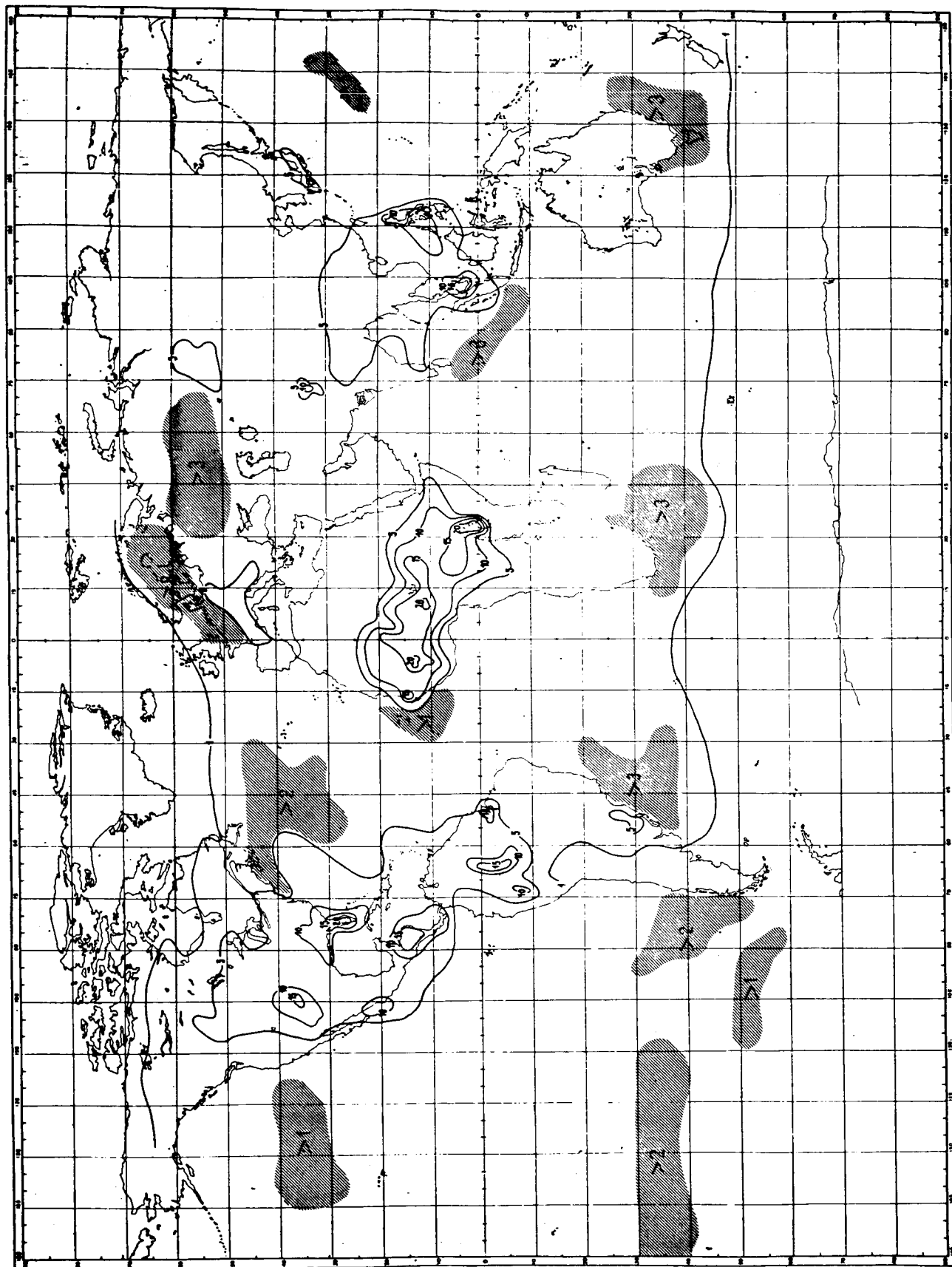
3.5 WORST CASE ESTIMATES

The preceding paragraphs have presented fairly precise composite reflectivity profiles for the summer of 1963 at Montreal, approximate profiles for continuous precipitation and estimates of worst likely profiles for thunderstorms. The latter come closest to the interest of the design engineer, so their use will be supported in the only way available, i.e., by demonstrating that the world's weather can be much more severe than was found at Montreal in 1963. Beyond this, there can only be a plea for more data of the same type, taken in more representative as well as extreme climates.

A general indication of the occurrence of thunderstorms is given in Figure 3-6 and 3-7, and several indices of severe weather are collected in Table 3-1 for Montreal in 1963 and for several places of interest, through the years. Miami has nearly an extreme climate for the United States, but certainly not in view of areas which may be of importance to future satellite communications. In the table, the quotient in the third line is included as being a commonly-used indicator of maximum rates of precipitation, and a rough correlation is indeed noted with the following three lines, although there is already for Nigeria an indication of the questions yet to be attacked regarding correlation of reflectivity profiles and other factors. A thunderstorm day is one on which an observer has reported a thunderstorm within sight of his station. It is known that thunderstorm height increases with latitude, but the question for $\int Z(h)dh$ has not been studied.

It is very difficult to evaluate Table 3-1 quantitatively. Quite arbitrarily one may note that several of the indices are 10 times those for Montreal and therefore expect only 10 dB

Figure 3-6. Thunderstorm Days - August



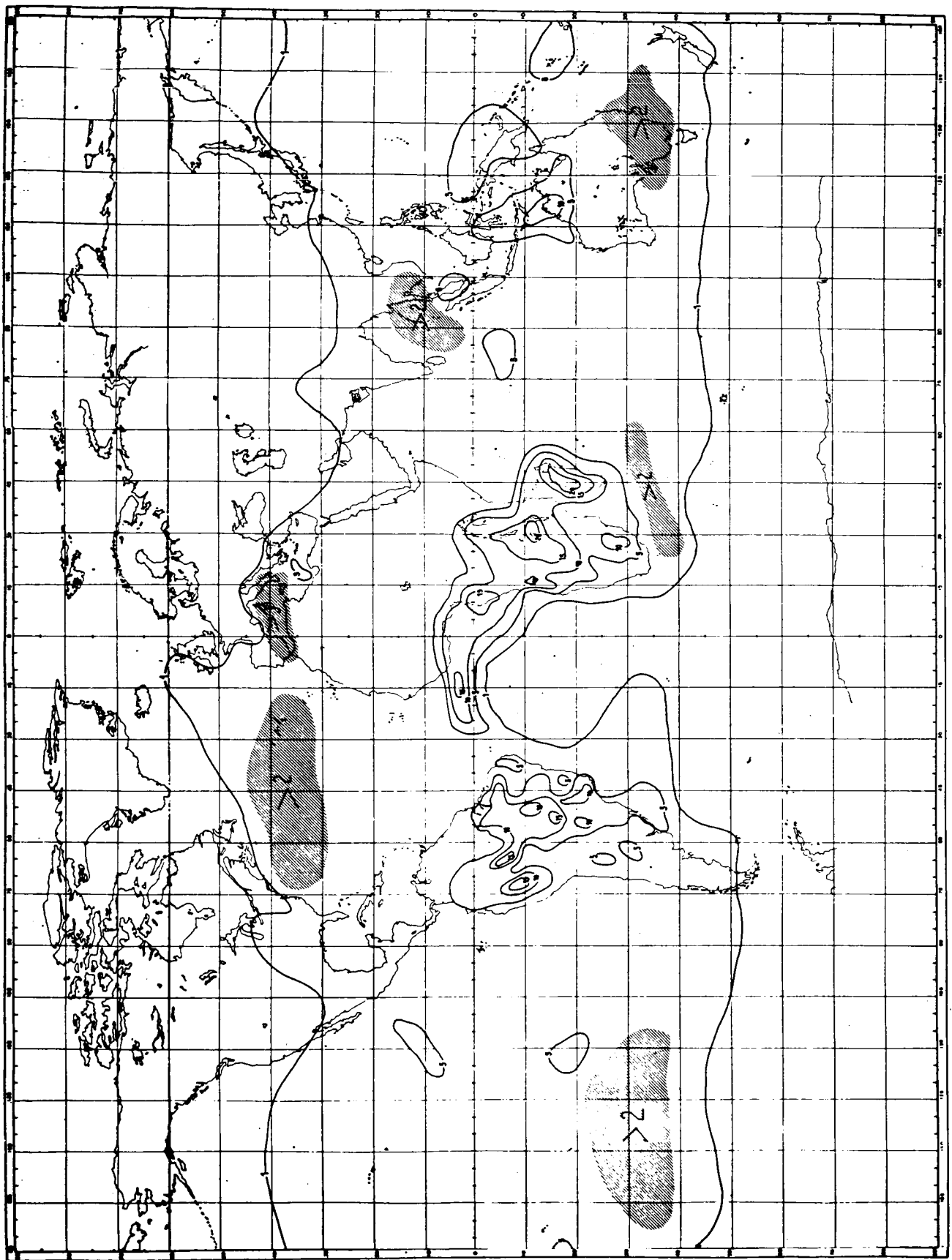


Figure 3-7. Thunderstorm Days - February

TABLE 3-1. SEVERE WEATHER INDICES

	Montreal		Washington, D.C.	Miami, Florida	Mamfe, Nigeria
	1963	Long Term			
<u>PPN in inches*</u>					
Avg. Annual		41	42	60	134
Days with 0.01"		157	124	135	192
Quotient		.26	.34	.44	.70
July Total	2.5	3.7	4.4	6.1	25
24-hour maximum	1.7	4.1	7.3	15.1	6.6
1-hour maximum	1.6	1.6	1.9	4.5	
<u>Thunderstorm Days**</u>					
Annual	21	20	37	58	201
Worst Month	6	5	9	11	30
<u>Echo Probability†</u>					
35-40,000 ft	8%	8	8	48	
55-60,000 ft		0.1%	0.1	1.0	

*From Tables of Temperature, Relative Humidity and Precipitation for the World, Part I, M.O.617a, Meteorological Office, except for Montreal 1963 from official monthly reports and 1-hour maximum from USWB.

**For U.S. from Reference 8, for Nigeria from World Distribution of Thunderstorm Days, WMO/OMM-No.21.TP. 21, for Montreal from official monthly reports.

†Within 100 miles of station in July from Horizontal and Vertical Distributions of Radar Echoes, by D. D. Grantham and A. J. Kantor, 12th Conference on Radar Meteorology, Norman, Okla., October 1966, pp. 500-505, except for Montreal 1963 from McGill University.

more interference at the worst possible time and place. There are, however, two reasons for rejecting this simple approach. First, none of the indicators is directly related to interference. For example, more thunderstorm days could imply larger, higher and stronger storms (true for Colorado Springs), with interference increasing as the square or cube of the ratio under study. Second, the problem concerns the return rate of infrequent but substantial events. That is, in much of the world, if a severe thunderstorm does produce interference in the beam of an earth station, it will be strong and probably considerably longer than the four minutes representing 0.01 percent of a month. Therefore, the estimated profiles may be used to indicate what almost certainly will happen in some year, but with an indefiniteness as to probability of occurrence in a given year which should be rectified by additional data as soon as possible.

SECTION 4

APPROXIMATE METHOD

4.1 CONCEPT

As the basic tools for solving the problem have been developed earlier, it is now appropriate to consider the presentation of solutions. This in itself is no small problem due to the large number of parameters involved. Explicitly, they are λ , k , $Z(h)$ and d in common, and b_{es} , b_{ts} , A_{es} , A_{ts} , E_{es} , and E_{ts} for the two stations. Now, it seems reasonable to set λ , k , $Z(h)$, b_{es} , and b_{ts} constant as they are in a sense non-geometrical, and changes in λ and b_{es} , at least, are easily accommodated. Further, as has been noted, E_{ts} is rarely over 3° , and E_{es} is often about 30° , so that values of 1° and 30° , respectively, are representative. This leaves d , A_{es} and A_{ts} to consider. In the case of intersecting beams, fixing any two of these determines the other one so that transmission losses may be plotted on the two-dimensional earth's surface. For non-intersecting beams, however, the factors are not conveniently interdependent so that full presentation becomes a formidable task, and the alternative of a manual calculation is impractical. Therefore, the simplified approach of Paragraph 2.4 is used.

Specifically, if the sidelobe pattern of the terrestrial radio-relay station antenna beam is to be considered, and it is of the essence when the beams are not intersecting, the effects of some other variables, such as the radio-relay station beam elevation, E_{ts} , and the azimuth of the earth-station beam, A_{es} , must be disregarded in a usable presentation. As it is clearly necessary to have some measure of the errors introduced by such approximations, it will now be shown that in most cases of interest the simple approach is useably accurate over a wide range of the suppressed variables. A program based on the precise Equations (2-13) and (2-14) has been used to check the effects of ignoring

A_{es} and E_{ts} in Equations (2-16) and (2-19) as d and A_{ts} are decreased. The gain g_{ts} , which away from the great-circle plane depends to a good approximation only on A_{ts} , and the elevation E_{es} are outside the integral in Equation (2-16) and can then be simply included in the computation.

4.2 TESTS

The checks were performed with $\lambda = 7.5$ cm, $k = 4/3$, an earth-station antenna with a diameter of 26 m (85 ft) and CCIR sidelobe envelope, and the TD-2 delay-lens antenna pattern of Figure 2-2. The first test assumed $D = 10$ or 100 km, $E_{ts} = 1^\circ$, and $A_{ts} = 20^\circ$ off the line between stations. For an earth-station elevation of 90° , the following values were found for p_r/p_t in decibels:

<u>D</u>	<u>APPROXIMATE</u>			<u>EXACT</u>		
	$(P_r - P_t)_{es}$	$(P_r - P_t)_{ts}$	$P_r - P_t$	$(P_r - P_t)_{es}$	$(P_r - P_t)_{ts}$	$P_r - P_t$
10	-149	-146	-145	-152.3	-149.3	-147.6
100	-170	-160	-160	-173.1	-163.2	-162.8

It can be seen that $(P_r - P_t)_{ts}$ is the controlling factor and that

in spite of the drastic assumptions used in Equation (2-19) and use of the Z value at the height of potential intersection of the two beams, the results are accurate within 3 dB. Table 4-1a indicates the errors resulting from use of different values of A_{es} and E_{es} , where low values of the latter tend toward beam intersections as indicated by the large errors at $E_{es} = 5^\circ$ and $A_{es} = 60^\circ$ and 90° . As the errors here are negative, it is seen that they represent approximate values minus true values. It should be noted that these errors are residuals, that is, values of p_r/p_t from Equation (2-16) have been multiplied by $\sin E_{es}$ and divided by g_{ts} before comparison with the exact values shown above. The table shows that accuracy is not significantly impaired with E_{es} down to 30° . If $E_{es} = 90^\circ$, and A_{ts} and E_{ts} are varied, Table

4-1b is found from comparison of the exact values with those computed from Equation (2-19) as these are found to be controlling. Here it can be seen that for any E_{ts} and A_{ts} greater than about 1° , useful accuracy is again preserved.

In view of the customary use of simplified antenna patterns and reflectivity models, it may be considered that the approximate method is about as good as the input data throughout the range of major interest, $E_{es} \geq 30^\circ$, $A_{ts} \geq 5^\circ$.

TABLE 4-1. ERRORS FROM GEOMETRICAL EFFECTS, IN DECIBELS

		(a)					
Rel. $A_{e s}$		0°	30°	60°	90°	180°	270°
<u>d</u>	<u>$E_{e s}$</u>						
100km	60°	+0.6	+0.5	+0.5	+0.5	+0.6	+0.6
	30°	+1.2	-0.2	-0.2	+0.1	+2.7	+2.6
	20°	+0.9	-1.5	-1.5	-1.1	+3.1	+4.1
	10°	+0.4	-4.1	-4.8	-4.9	+6.4	+6.2
	5°	+0.4	-7.8	-14.3	-15.2	+8.7	+8.4
10km	60°	+0.1	0	0	-0.1	+0.6	+0.6
	30°	+0.8	-1.0	-1.1	-0.9	+2.4	+2.5
	20°	-0.3	-1.9	-1.9	-1.7	+3.5	+3.9
	10°	-1.3	-3.2	-4.1	-4.8	+5.6	+6.3
	5°	-2.3	-6.0	-12.5	-13.3	+8.0	+9.0

		(b)		
Rel. $A_{t s}$		2°	4°	6°
<u>d</u>	<u>$E_{t s}$</u>			
100 km	2°	0	-2	-3
	1°	+2	-1	-2
	0°	+2	-2	-3
10 km	2°	-2	-2	-1
	1°	-2	-2	-1
	0°	0	-3	-3

SECTION 5

RESULTS

5.1 INTERSECTING BEAMS - LOSS CONTOURS

A computer program based on Equation (2-13) has been used to produce Figure 5-1, for $\lambda = 5$ cm, $k = 4/3$, and $b_{ts} = 2^\circ$, corresponding to a 6-foot diameter terrestrial station paraboloidal antenna. This is a plan view, looking down at the earth, showing an earth station located with its antenna beam directed to the right and elevated 3° or 30° . At any point on the earth, a radio-relay station is assumed to be located with its beam aimed toward the lowest intersection with that of the earth station. The contours are isopleths of transmission loss, $P_r - P_t = 10 \log (p_r/p_t)$, in decibels, for 0.02 percent of the worst month of one summer at Montreal. Approximate figures may be obtained for some other percentage S by adding $12 \log (.02/S)$, thus the interference is less for the higher percentages. Similarly, adjustments may be made for other values of λ and b_{ts} by reference to Equation (2-13). Higher values of E_{ts} increase the loss, and b_{es} has no effect in the horizontally uniform medium assumed. It may be noted that the shape of the contours is controlled largely by the inverse sine of the angle between the beams as shown in Equation (2-7a), so that the separation for constant loss increases as the beams become more nearly parallel, even behind the earth station at short ranges.

For an earth station with an antenna elevation of 30° or more, its antenna beam leaves the atmosphere, assumed to be 20 km thick, no farther than 35 km horizontally from the station, so that $d_{ts} = d$ approximately. Further, the maximum change in $\sin \theta$ in moving around the station is only about 3 dB. Therefore the contours are very closely circles such as would be found for a vertical beam, confirmed by the computer in the lower half of Figure 5-1.

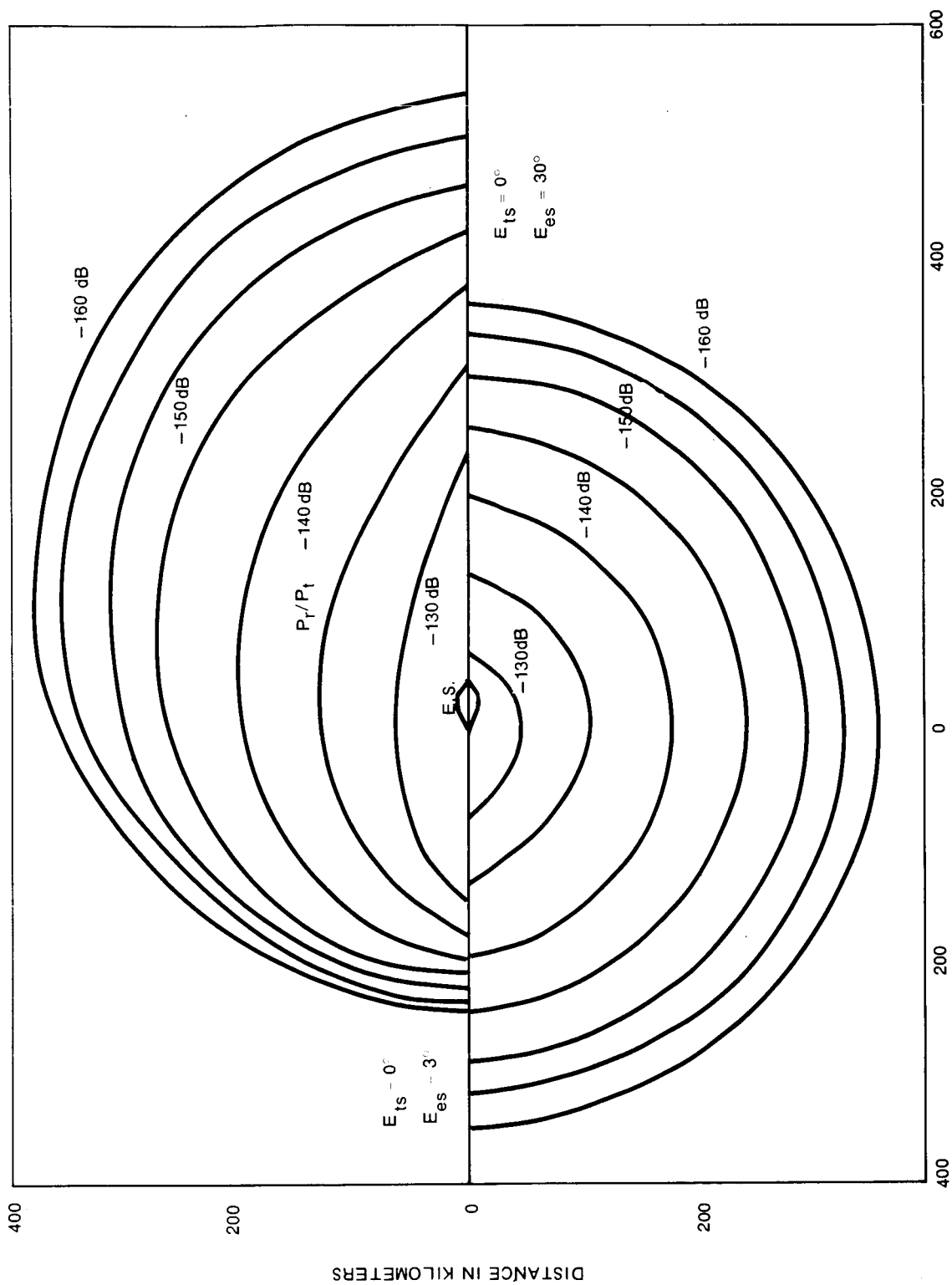


Figure 5-1. Loss Contours for Intersecting Beams

5.2 INTERSECTING BEAMS - LOSS PROFILES

As Figure 5-1 covers a very limited range of variables, both geometrical and meteorological, a fairly general method for manual computation is also offered, based on the bilinear reflectivity profile for Montreal. It will be used first to derive values for comparison with Figure 5-1 and then to show the effects of changing the effective radius of the earth, et cetera.

Using the method of Paragraph 2.2, with $b_{ts} = 2^\circ$ and $E_{es} = 30^\circ$,

$$\begin{aligned} h_b &= D/115 & \text{at } \theta &= 90^\circ \\ &= D/57.3 & \text{at } \theta &= 0^\circ \text{ or } 180^\circ \end{aligned}$$

Intersection heights may be found from Figure 5-2, a plot of $h = D^2/17,000 + D E_{ts}$ with h and D in kilometers. From Equation (2-7), the curve marked $E_{ts} = 0^\circ$ of Figure 5-3 may be found, agreeing fairly well with the lower half of Figure 5-1.

The effects of several changes are also shown on Figure 5-3. The curve for $E_{ts} = 2^\circ$ indicates the reduction of interference from the higher common volume. The curve for $h_{ts} = 0.1$ km reflects the fact that an elevated terminal can see, at longer ranges, the lower, steeper portion of the bilinear profile, with a larger effective Z .

Similarly the curves for $k = 2.8$ and $k = \infty$ show the effect of super refraction and ducting, which lower the common volumes considerably at very long ranges. Table 5-1 (Reference 13) indicates the occurrence of both, although this table must be used with caution, as thunderstorms are unknown in the Antarctic and may not occur at the same time as ducting in Saigon. There is reason from page 22 of Reference 3 and elsewhere (Reference 1) to believe that there is some correlation, but the matter has not yet been pursued.

All of the preceding curves are based on the Montreal 1963 composite statistical data, so it must be recognized as indicated

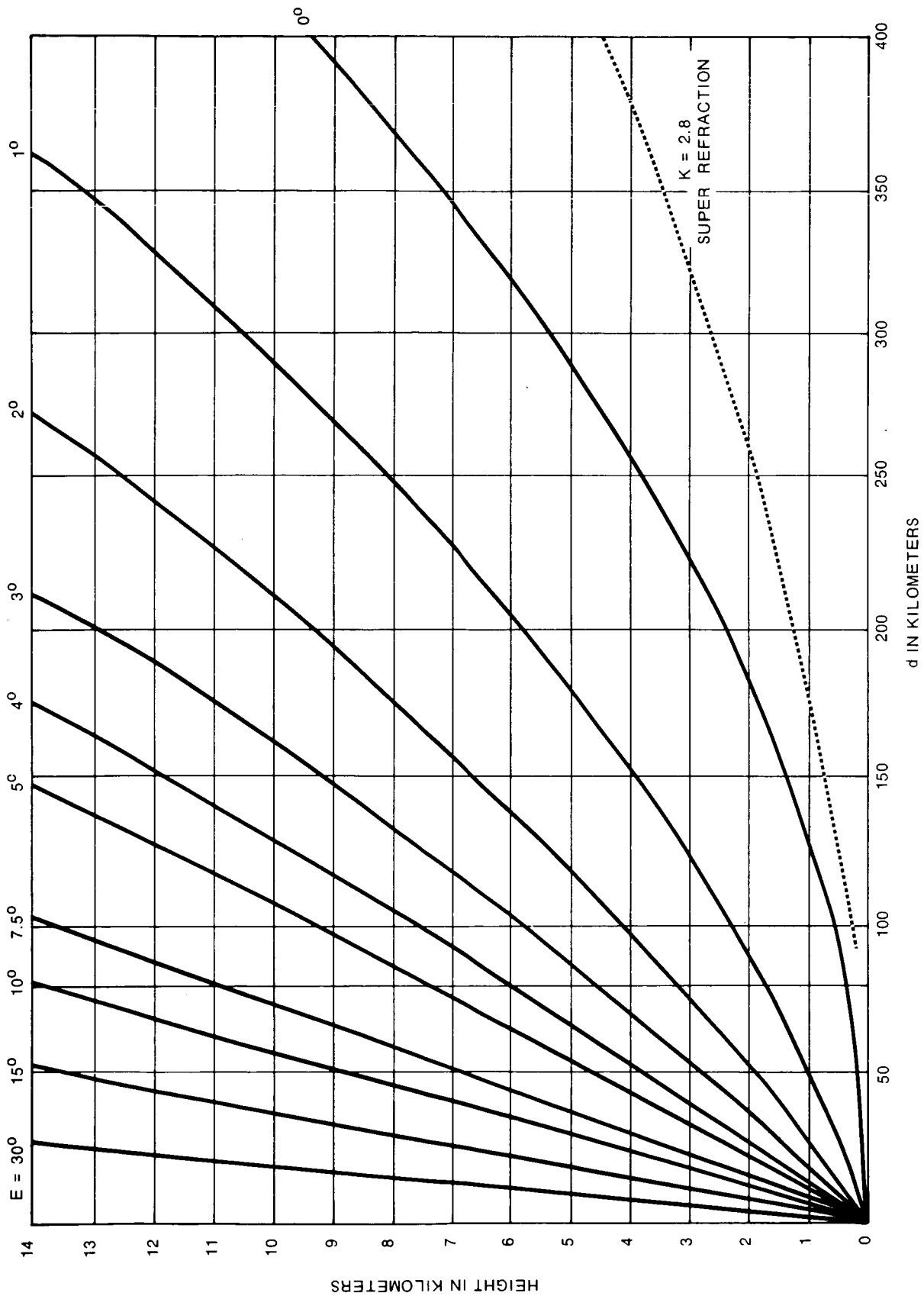
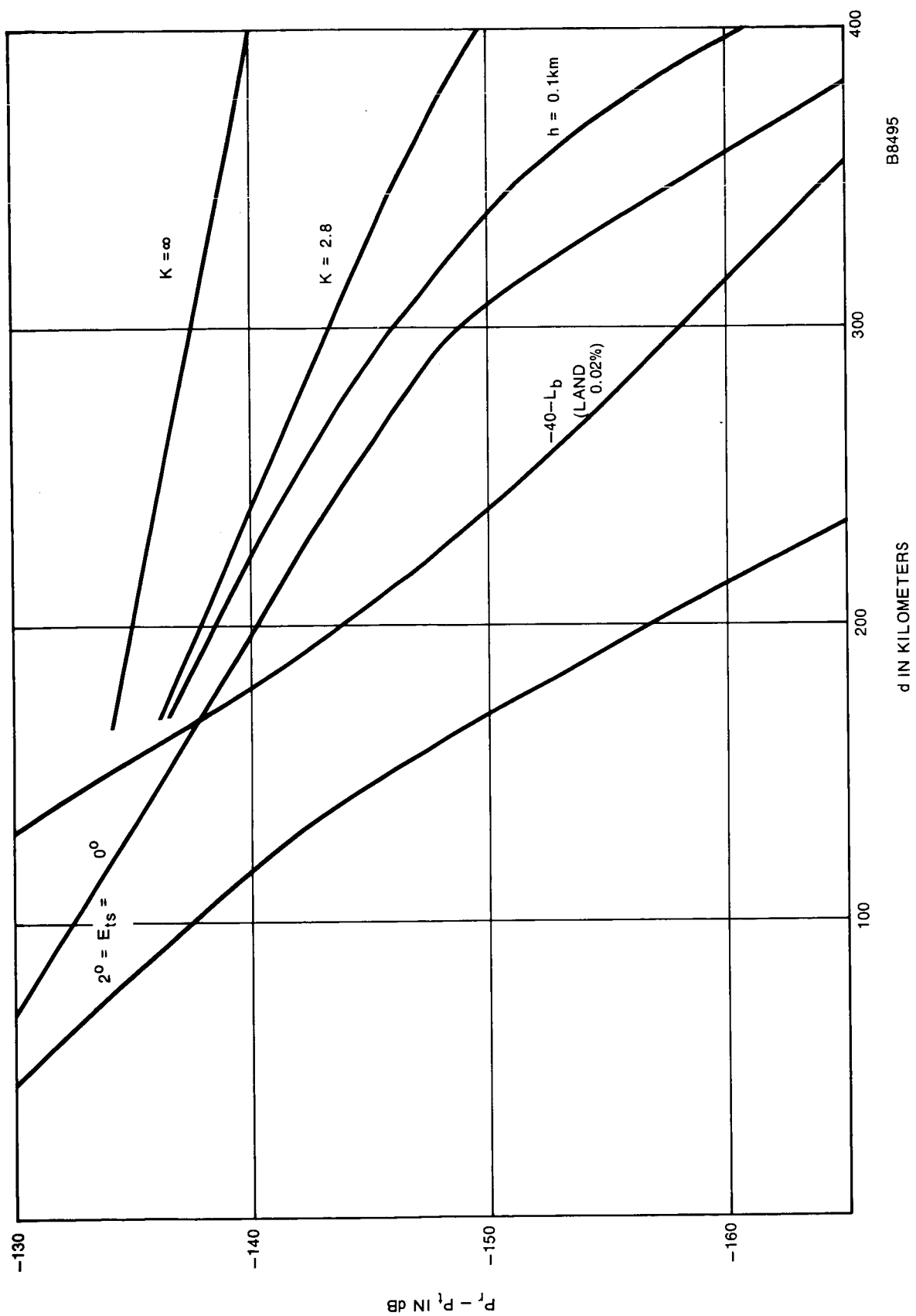


Figure 5-2. Effects of Earth's Curvature



B8495

Figure 5-3. Loss Profiles for Intersecting Beams

TABLE 5-1. PERCENTAGES OF TIME INITIAL REFRACTIVITY GRADIENTS ARE EXCEEDED

Climate	Place	Month	Super refraction (N/km \leq - 100)	Ducting (N/km \leq 157)
<u>Temperate</u>				
Marine	Bordeaux, France	August	33	10
Continental	Moscow, U.S.S.R.	August	1	--
Mediterranean	Nicosia, Cyprus	August	20	10
Arctic	Antartica	August	85	55
<u>Tropical</u>				
Wet	Saigon, Viet Nam	August	35	10
Dry	Aoulef, Algeria	February	3	1
West Coast	Dakar, Senegal	February	79	67

in Paragraph 3.5 that the interference may be considerably worse at different times and places. As thunderstorms are very erratic in most temperate climates, it is of interest to note that the effect of continuous rain of 50 mm/hr, using the method of Paragraph 3.2, is about that for $E_{ts} = 0$, out to 250 km where it falls off sharply because of its limited extent in height. Table 3-1 indicates the likelihood of such a rainfall rate for one hour of any year in a rainy climate, and for more than 0.01 percent of a month or four minutes in most (Reference 8).

The curve marked 40 - L_b represents typical transhorizon loss along a great-circle path over land, found from the propagation curves of Rec. 1A of the Final Acts of the EARC (Geneva, 1963) or CCIR Doc. IV/1022 (1963-1966). The governing equation is

$$P_r - P_t = G_t + G_r - F_s - L_b \quad (5-1)$$

The radio-relay antenna is considered aimed at the earth station with its gain, G_t , taken as 40 dB. Even if it is aimed off and may be considered only isotropic ($G_t = 0$), precipitation scatter is still important for paths over the sea. The horizontal gain of the earth-station antenna, G_r , is taken as zero for elevations higher than 19° , a modification of the pattern recommended in CCIR Doc. IV/1010 (1963-1966):

$$G = 32 - 25 \log \theta^\circ \quad (5-2)$$

For lower elevations, of course, the curve marked 40 - L_b moves up. The site-shielding factor, F_s , moves the curve down to reduce interference and will be effective against continuous rain and the composite profile leading to curves such as $E_{ts} = 2^\circ$, unless offset by refraction. This effectiveness will be illusory, however, against a severe storm in the common volume, in which large scattering particles may be found up to great heights.

5.3 NON-INTERSECTING BEAMS

The geometry of the common volume of two intersecting beams is relatively simple compared to that of the two extensive beams involved in the non-intersecting case. It can be seen, for example, that if the high-elevation earth-station antenna beams of a regional distribution system are of special interest, they are in a sense matched to vertically-developed thunderstorms of small horizontal extent, but not to low-lying, extensive, stratiform rain. On the other hand, the low-elevation earth-station antenna beam of an intercontinental communication system will be far more concerned with the latter than with the former. The terrestrial station radio-relay beam is also chiefly concerned with the stratiform rain; therefore it is necessary to consider both beams in specific cases.

These two points may be illustrated by calculations using Equations (2-22) and (2-24) and the following assumptions:

$$\begin{array}{ll} \lambda = 5 \text{ cm} & E_{es} = 90^\circ \text{ (Beams perpendicular)} \\ d = 10 \text{ km} & = 10^\circ \text{ (Beams roughly parallel)} \\ b_{ts} = 2^\circ & \alpha_{ts} = 20^\circ \end{array}$$

Thunderstorm $Z = 6 \times 10^5$, constant to $h = 10 \text{ km}$ with radius, u , of 1.5 km

Continuous rain $Z = 6 \times 10^5$, constant to $h = 2 \text{ km}$, infinite in horizontal extent

Using Equations (2-22) and (2-24)

$$p_r/p_t = 1.25 \times 10^{-16} Z_o (s/y^2 + 1/y) \quad (5-3)$$

where $s = 1000 h/\sin E_{es}$ for continuous precipitation with $h =$ height of precipitation in kilometers. For thunderstorms of radius u kilometers, located for maximum effect,

$$s = 2000u/\cos E_{es} \text{ if } E < \sin^{-1} h/2u \quad (5-4a)$$

$$\text{or } s = 1000h/\sin E_{es} \text{ if } E > \sin^{-1} h/2u \quad (5-4b)$$

and the term $1/y$ should be multiplied by $(1/90) \tan^{-1}(1000u/y)$.

The results are as follows in decibels:

	E_{es}	$(P_r - P_t)_{es}$	$(P_r - P_t)_{ts}$	$P_r - P_t$
TST	90°	-132	-143	-130
	10°	-136.5	-143	-136
Cont.	90°	-139	-136.5	-135
	10°	-131.5	-136.5	-131

As expected the high beam produces more interference in the thunderstorm than the low does, and vice versa.

It may be noted that for the two worst cases, $(P_r - P_t)_{ts}$ may be ignored and that the same equation applies,

$$p_r/p_t = 1.25 \times 10^{-16} Z_e \left(\frac{1000h}{y^2 \sin E_{es}} + \frac{1}{y} \right) \quad (5-5)$$

If arbitrarily $h/\sin E_{es}$ is taken as 20 with $Z_e = 3 \times 10^5$, and if it is agreed that p_r/p_t should be no more than 10^{-14} then y is found to be 9,400 meters or about 6 miles. This represents the closest permissible approach between the terrestrial beam axis and the earth-station beam which has practically zero width. Alternatively, if it is necessary to locate an earth station among many terrestrial stations, their beams may be plotted on a map assuming a width of 12 miles and the space between them considered as possible sites for the earth station. The first-order result must be modified by consideration of earth-station beam orientation, terrestrial station beam height near the chosen site and approximate values of Z_e and h , but it does provide the desired rough guide for avoiding harmful interference.

5.4 CONCLUSIONS

It has been shown in the preceding discussion that non-intersecting beams are not likely to produce harmful interference without a severe combination of small separation, stormy weather, or low tolerance such as for a station in the manned space service. For intersecting beams, on the other hand, relatively mild weather and large tolerances may result in undesirable interference at hundreds of kilometers separation. This brings about a very peculiar situation.

By definition, coordination distance calculations must be simple, ignoring radio-relay antenna azimuths. Yet in most climates, not only can serious interference arise or be caused in a region outside the coordination distance, but also any site shielding, such as that used at Andover and other stations to limit the distance, may be ineffective. There is, however, some measure of protection against this problem when coordination of a station in the space communication service is performed for a wide range of azimuths, and down to a low elevation. This extends the process to a wide region likely to contain most of the sources of precipitation scatter interference and generally causes avoidance of concentrations of population and radio-relay stations. On the other hand, some current proposals for television relay by satellite envision earth stations close to each of hundreds of existing television broadcast stations whose locations, based on potential customers, correlate closely with population centers and their attendant microwave communication complexes. In this case it is likely that coordination for a narrow range of azimuths and elevations will be sought for two reasons: the necessity of aiming at only a short portion of the stationary orbit and the requirement of avoiding interference to a relatively large number of radio-relay stations. It is this latter avoidance which may be rendered entirely illusory by precipitation scatter from far off the usual great-circle paths. Therefore, it is suggested when coordination is being initiated for less than hemispheric coverage, that Figure

ACKNOWLEDGEMENT

The assistance of A. Cohen and J. Ruttenberg in geometrical analysis and computer programming is gratefully acknowledged, as well as the careful review and useful suggestions of W.I.Thompson,III, of NASA.

5-1 be used as a rough indication of the region within which radio-relay stations may interfere, with consideration given to the relative severity of storms and the nature of the earth station. Then the criteria of Paragraph 5.3 should be applied. This procedure can be made more definite and effective after a review of available climatological and weather radar data.

REFERENCES

1. Doherty, L. H. and Stone, S. A., "Forward Scatter from Rain," Trans. IRE, AP-8 (July 1960).
2. Dennis, A. A., "Precipitation Scatter as an Interference Source in Communication Systems," IRE Convention Record, Part I, Antennas and Propagation, p. 145 (1962).
3. Culnan, D. E., et al, "Radio Scattering Cross Sections of Thunderstorms," NBS Report 8816, June 9, 1965. (Unpublished)
4. Probert-Jones, J. R., "The Radar Equation in Meteorology," Quarterly Journal of the Royal Meteorological Society, Vol. 88, No. 378, October 1962, p. 485.
5. Curtis, H. E., "Radio Frequency Interference Considerations in the TD-2 Radio Relay System," B.S.T.J., 39, March 1960, p. 369.
6. Battan, L. J., Radar Meteorology, University of Chicago Press, Chicago, 1959.
7. Atlas, David, "Model Atmospheres for Precipitation," Handbook for Geophysics and Space Environments, Section 5.2, p. 5-6, (1965).
8. Bussey, H. E., 1950, "Microwave Attenuation Estimated from Rainfall and Water Vapor Statistics," Proc. Inst. Radio Eng., Vol. 38, p. 781.
9. Byers, H. R. and Braham, R. R. Jr., The Thunderstorm, Government Printing Office, 1949.
10. Donaldson, Ralph J. Jr., "Radar Reflectivity Profiles in Thunderstorms," Journal of Meteorology, Vol, 18, No. 3, June 1961, pp. 292-305.
11. Hamilton, P. M., "Precipitation Profiles for the Total Radar Coverage," McGill University Stormy Weather Group Scientific Report MW-37, September 1964.
12. Marshall, J. S., Holtz, C.D., and Weiss, Marianne, "Parameters for Airborne Weather Radar," McGill University Stormy Weather Group Scientific Report MW-48, May 1965.
13. Cahoon, B. A., and Thayer, G. D., "Worldwide Occurrence of Superrefractive and Ducting Conditions Affecting Radio Frequencies," NBS Report 8864, August 1965.

APPENDIX A
COMPUTATION OF TRANSMISSION LOSS

A program has been written to compute precipitation scatter transmission loss with specific application to the problem of most concern, that of an earth station aimed at a satellite anywhere in the stationary orbit. The problem under consideration is the expected interference to the Rosman, N.C., earth station from a large group, but by no means all, of the radio-relay stations of interest, as shown on Figure A-1. The broad lines are state boundaries. The thin solid lines are 4-GHz links, the dashed, 6 GHz. Rosman is shown by a star. Only links oriented toward Rosman were selected for study.

A program called NEWAZ finds for the earth station, and each terrestrial radio-relay station, which stationary satellite longitude produces a beam intersection, giving also beam intersection height and earth-station azimuth and elevation. The results are passed on to and printed by the next program as shown in Figure A-2.

AZNEW uses the preceding data to compute the transmission loss via precipitation scatter. Other inputs are:

- a. Ratio of effective to true earth's radius, K (= 1.33)
- b. Maximum height of precipitation, TOP (= 20 km)
- c. Maximum height of intersection used, H (= 66 KFT)
- d. Wavelength, L (= 7.5 cm)
- e. Number of slices added, N (= 20)
- f. Reflectivity profile Z (= Montreal 1963)
- g. Terrestrial station antenna pattern, GAIN TS (= Delay Lens TD-2)

- h. Earth-station beamwidth, BW ($= 0.14^\circ$)
- i. Earth-station antenna pattern, GAIN ($= \text{CCIR} = 32-25 \log \alpha^\circ$)

The outputs include (angles in degrees and minutes):

- a. Earth-station latitude, longitude, azimuth to intersection if above 5° in elevation, otherwise nearest of 100° or 260° to intersection. In the latter cases elevation used is 5° . Elevation of intersection or NO SOLUTION.
- b. Terrestrial station latitude, longitude, azimuth and elevation.
- c. Longitude of satellite causing intersection.
- d. Interference $P_r - P_t$ in decibels
dB = total of:
PR = effect of sidelobes of terrestrial antenna
CI = effect of sidelobes of earth-station antenna

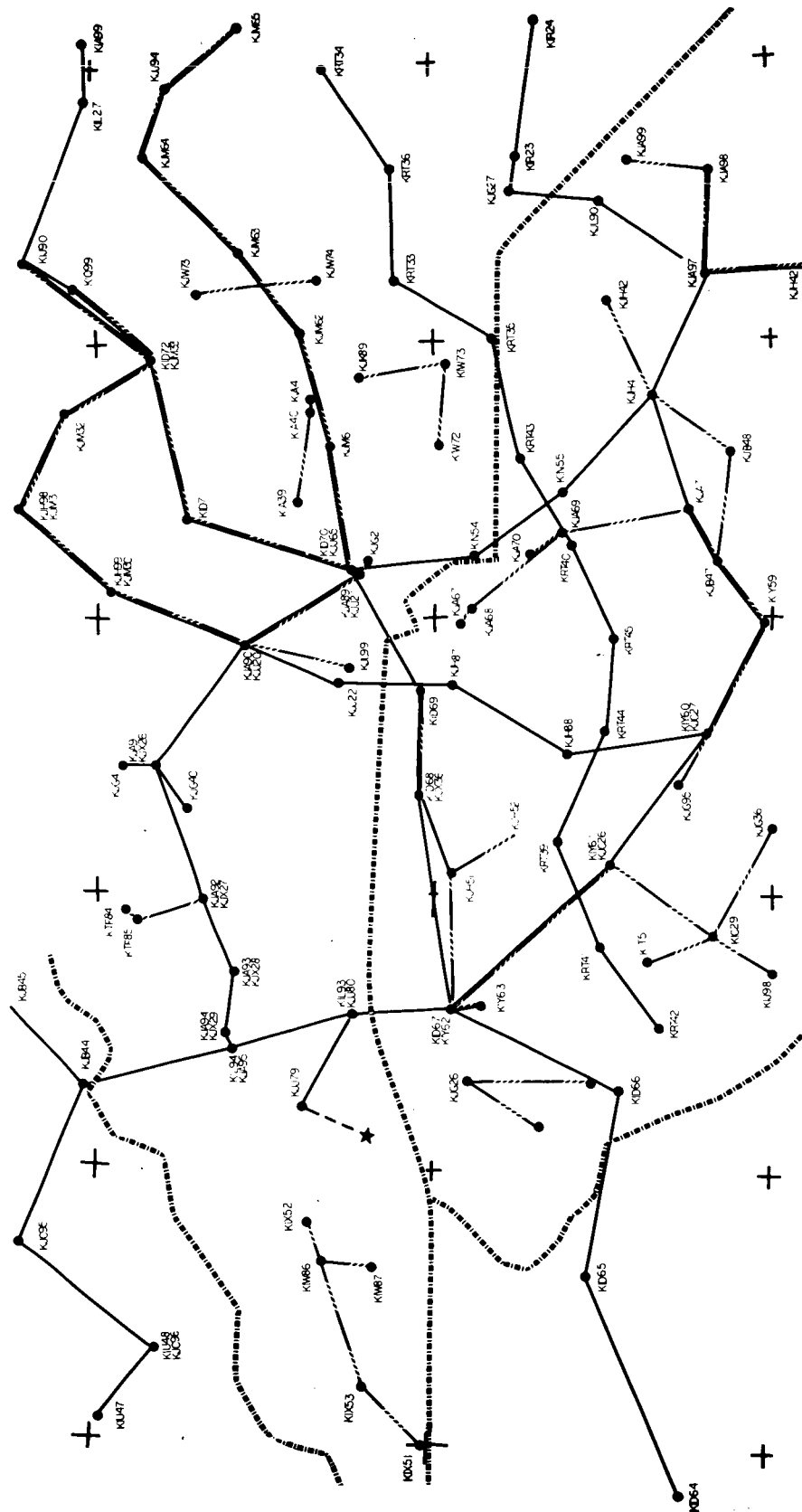


Figure A-1. Rosman, North Carolina Area

AZNEW 15:55 WS WED 03/08/67

IN SUBSJR
IN .FIRST
IN PRPT
IN .FIRST

? 0.25,1.25

K=1.33 TOP= 20.KM H= 20.KM WL= 7.5CM N= 20. Z=M GAINTS=DL

EARTH STATION LAT.= 35.19 , LON.= -82.87 BW= .14 GAIN=CCIR

.....

TERRESTRIAL IDENT.	RADIO--RELAY LAT LONG	STATION AZIM	ELEV	XSECT HT-KM	EARTH STATION AZIM ELEV	SAT LONG
KID 69	35 2' -81 15'	270 28'	.00	4.4	260 0' 1 33'	-160 17'
	DB=-149.5	PR=-149.6	CI=-165.4			
KID 72	35 50' -80 3'	257 57'	.00	11.7	260 0' 3 3'	-158 26'
	DB=-163.4	PR=-164.2	CI=-171.5			
KIR 23	34 44' -79 20'	286 1'	.00	11.7	N O	S O L U T I O N
KIR 24	34 41' -78 51'	278 46'	.00	6.1	101 32' 7 11'	-12 22'
	DB=-131.3	PR=-152.1	CI=-131.4			
KIU 47	35 58' -83 55'	127 14'	.00	1.3	100 0' 3 11'	-7 28'
	DB=-136.1	PR=-136.1	CI=-162.7			
KIY 59	34 0' -81 1'	299 13'	.00	3.8	260 0' 3 47'	-157 32'
	DB=-145.0	PR=-145.0	CI=-171.9			
KIY 60	34 11' -81 24'	306 17'	.00	2.0	258 36' 7 0'	-153 36'
	DB=-138.2	PR=-142.1	CI=-140.4			
KIY 61	34 28' -81 52'	317 18'	.00	.7	100 0' 1 59'	-5 59'
	DB=-135.3	PR=-135.9	CI=-144.1			
KJA 91	35 49' -81 32'	235 23'	.00	1.0	100 0' 3 23'	-7 42'
	DB=-134.3	PR=-135.9	CI=-139.2			
KJA 97	34 11' -79 46'	294 40'	.00	3.6	100 0' 3 15'	-7 33'
	DB=-143.1	PR=-143.7	CI=-151.7			
KJM 61	35 18' -80 22'	261 16'	.00	1.3	100 0' 0 38'	-4 19'
	DB=-147.9	PR=-149.4	CI=-153.1			
KRT 36	35 7' -79 23'	269 23'	.00	10.1	259 42' 5 33'	-155 23'
	DB=-169.4	PR=-170.6	CI=-175.5			
KRT 44	34 29' -81 24'	293 45'	.00	2.0	260 0' 3 15'	-158 12'
	DB=-139.2	PR=-139.2	CI=-166.1			

Figure A-2. Computer Printout